International Symposium
On Turbulence and Shear Flow
Phenomena (TSFP-9)
June 30 - July 3, 2015 *Melbourne, Australia*

DNS OF TURBULENT JETS ISSUING FROM ACOUSTICALLY LINED PIPES AT DIFFERENT MACH NUMBERS

Richard D. Sandberg[1], **Brian J. Tester**[2]
[1]Aerodynamics and Flight Mechanics Research Group, [2]Institute of Sound and Vibration
Faculty of Engineering and the Environment, University of Southampton
Highfield, Southampton, SO17 1BJ, U.K.
sandberg@soton.ac.uk, b.j.tester@soton.ac.uk

ABSTRACT

A series of Direct Numerical Simulations (DNS) was performed of fully turbulent jets with a target Reynolds number, based on nozzle diameter, of $Re_{jet} = 8,000$. The simulations included a long pipe in order to let the flow develop to a fully turbulent state before exiting into a laminar co-flow, and in order to ensure that all possible noise generation mechanisms are represented. Particular attention was paid to minimizing internal noise in the pipe as it was shown in previous studies to contaminate the overall far field noise and make the study of jet-mixing noise difficult. This was achieved by including liner boundary conditions inside the pipe and by modifying the turbulent inflow boundary condition of the pipe. The sound radiation from the pipe/jet configuration was decomposed into its azimuthal Fourier modes and analyzed using a phased array source breakdown technique in order to separate sources associated with jet noise mechanisms from additional noise sources that can be attributed to internal noise or unsteady flow past the nozzle lip. The behaviour of the jet noise source was then studied as a function of jet exit Mach number. Using this approach, we were able to establish the Mach number scaling of the individual azimuthal Fourier modes of far field pressure for the jet mixing noise component.

INTRODUCTION

The need to control (reduce) jet noise is most pressing for the take-off stages of aircraft operation and it is important to understand the influence of forward flight on jet noise generation mechanisms. Early experimental research showed that jets in flight conditions are quieter compared to the same jets in a static environment (see, e.g., Crighton *et al.*, 1976; Tanna & Morris, 1977) and a number of theoretical and semi-empirical corrections to account for the flight conditions have been derived (c.f., Michalke & Michel, 1979*b*,*a*). These corrections can be used to obtain reasonable predictions of the noise levels, and it has been shown that the pressure power spectral density (PSD) for a co-flowing jet at 90° should scale with $(u_{CL} - u_{co})^5 u_{CL}^3$, where u_{CL} and u_{co} are the jet-exit centreline and co-flow velocities, respectively. Thus the velocity scaling shows a considerable dependence on the co-flow velocity.

However, it is not clear whether this velocity scaling applies only to the overall PSD or whether it also applies to different frequency ranges and individual azimuthal modes of the jet noise. To address this lack of detailed understanding has become even more important in current jet noise research, where the error bars in measurements of jet noise have become smaller and high quality simulations are able to match experimental data within 2-3dB (see, e.g., Bogey *et al.*, 2011). The lack of a fundamental understanding of the differences between noise sources in static and flight conditions is also a barrier when it comes to extrapolating the results of noise control strategies (such as microjets/chevrons) to flight conditions, as was clearly demonstrated in recent work by Shur *et al.* (2010), in which the efficiency of a microjet noise reduction concept in static and flight conditions was examined.

Therefore, to get further physical insight into the dominant jet noise generation mechanisms and velocity scalings for varying jet exit and co-flow velocities, it is desirable to obtain high-fidelity data of both the hydrodynamic and acoustic fields of the jet simultaneously. For the results to be reliable, however, it is important that the simulated jet captures all relevant mechanisms. It is well known that several different sources contribute to the overall sound radiation from subsonic jets: (i) large scale structures mainly occurring close to the potential core region, (ii) breakdown of large scale structures into fine-scale turbulence near the end of the potential core, (iii) fine-scale turbulence within the initial shear layers of fully turbulent jets, and (iv) trailing-edge noise resulting from the interaction between flow and the solid wall at the nozzle exit. Furthermore, the importance of the initial conditions on the jet development and noise has been well documented (Hussain & Zedan, 1978; Gutmark & Ho, 1983; Zaman, 1985; Raman *et al.*, 1989; Bogey & Bailly, 2010). Thus, to capture the above mentioned noise generation mechanisms and to consider realistic initial conditions for the jet, simulations in which the nozzle is included and the flow exiting the nozzle is fully turbulent are required. This configuration was considered by Sandberg *et al.* (2011), who simulated turbulent flow exiting a pipe into a laminar co-flow for three subsonic jet Mach numbers and varying co-flows, using direct numerical simulation (DNS) to eliminate uncertainties associated with turbulence modelling.

However, subsequent studies of this data using phased-array techniques found that the original DNS were contaminated by high levels of internal noise, generated within the pipe, and that it was difficult to extract the jet mixing noise, in particular for the axisymmetric mode (Sandberg & Tester, 2012; Tester & Sandberg, 2013). Therefore, a new set of DNS were performed with several vital

Jet Mach number	$R0$	$X1$	$X2$
0.46	4	6.28	−6.28
0.64	4	0.38	−15.07
0.84	4	1.177	−33.49

Table 1. Liner coefficients for all jet Mach numbers.

modifications, most noteworthy an explicit elimination of fluctuations in the axisymmetric mode of the turbulent inflow generation, and the use of an acoustic liner boundary condition for the inside of the pipe. In a precursor study, an acoustic liner model based on an impedance boundary condition was shown to be effective at removing acoustic fluctuations within the pipe without affecting the turbulent flow field (Olivetti *et al.*, 2015). The first analysis of the new DNS data has shown that the change in inflow boundary condition is largely responsible for reduction of internal noise of the axisymmetric mode, while the main role of the acoustic liner is the absorbtion of internal noise for higher azimuthal modes (Sandberg, 2014). The main focus of the current paper is on using a source breakdown technique, based on a phased-array approach, to establish the Mach number scaling of individual azimuthal Fourier modes of far-field pressure for the jet mixing noise component.

NUMERICAL SETUP

Direct Numerical Simulation Code

The compressible Navier–Stokes equations for conservative variables are solved in cylindrical coordinates using a mixed finite-difference/spectral code. The general numerical details and validation of the code can be found in Sandberg *et al.* (2015) and specific details concerning the current pipe/jet set-up have been reported in Sandberg *et al.* (2012).

A time-domain impedance boundary condition based on a mass-spring-damper analogy has been used, as defined by Tam & Auriault (1996). It can be written in the form where the generic resistance parameter $R0$ is identified as the dissipative term of the mass-spring-damper model and the two reactance parameters are identified as mass-reactance $X1$ and stiffness $X2$, which are chosen to produce resonance at the required Strouhal number. For the different jet Mach numbers, the liner parameters were set as listed in table 1. Preliminary studies showed that the liner boundary condition was not effective in removing acoustic radiation of the axisymmetric mode $m = 0$ at low Strouhal numbers. Therefore, the perturbation velocities of $m = 0$ are explicitly set to zero at the pipe inlet, thus eliminating mass flow fluctuations in the pipe. Removing velocity fluctuations in $m = 0$ was found to have no effect on the developed pipe flow downstream.

Simulation Geometry and Grid

The computational domain is composed of seven blocks, as shown in Fig. 1: flow inside the pipe (block 1), jet development downstream of the pipe exit (blocks 2, 3, 4 and 6), and coflow and acoustic field upstream of the pipe exit (blocks 5 and 7).

In the azimuthal direction 64 or 8 Fourier modes corresponding to 130 or 18 collocation points were used in the turbulent flow (blocks 1 to 5) and acoustic regions (blocks 6 and 7), respectively, resulting in a total of 225×10^6 grid

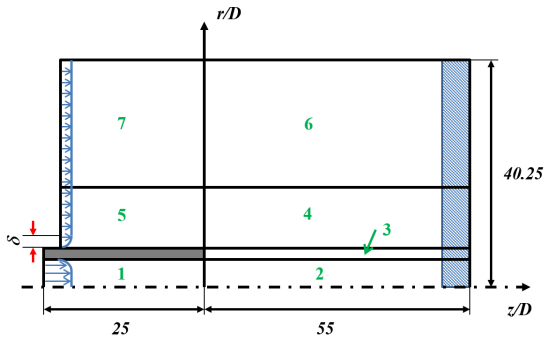

Figure 1. Sketch of the computational domain; the shaded region at the outflow denotes the region in which the zonal characteristic boundary condition (Sandberg & Sandham, 2006) was applied.

Case	M_{jet}	T_w	M_{co}	u_{CL}	Re_{jet}
M8c2L	0.8	1.14	0.2	1.27	7,700
M8c1L	0.8	1.14	0.1	1.27	7,700
M62c15L	0.62	1.08	0.15	1.35	8,523
M45c1L	0.45	1.04	0.11	1.14	7,409

Table 2. Simulation parameters; M_{jet}, M_{co} based on bulk velocity in nozzle, u_{CL} centreline velocity normalized with bulk velocity, Re_{jet} based on u_{CL}, nozzle diameter and kinematic viscosity at pipe wall. Mach numbers based on reference speed of sound using wall temperature T_w.

points. Fig. 1 also shows the dimensions of the computational domain, determined from preliminary turbulent pipe and jet simulations (Sandberg *et al.*, 2012). The finest grid spacing was $\Delta z/D = 0.0045$ and $\Delta r/D = 0.00129$ at the nozzle exit and the upper bounds of $\Delta z/D = 0.0515$ and $\Delta r/D = 0.0711$ were chosen to resolve acoustic waves up to Strouhal number $St_D \approx 2$ (based on the jet velocity and diameter) with at least 10 grid points.

A laminar boundary layer (Blasius solution) was prescribed at the inflow boundary on the pipe outside, reaching $\delta/D = 0.025$ at the jet exit. At the outflow boundary a zonal characteristic boundary condition was applied (Sandberg & Sandham, 2006), while characteristic boundary conditions were used at the upper freestream boundary.

Four different cases were conducted (Tab. 2), all using acoustic liner conditions inside the pipe, to study the Mach number scaling effect of the jet mixing noise for higher azimuthal modes. The changes in density and temperature were less than 15% of the wall values, with the wall set to be isothermal at the adiabatic temperature (T_w given in Tab. 2). All DNS were run for 150 nondimensional time units (based on diameter and bulk velocity inside the pipe) to allow the initial transients to leave the domain. Each case was then continued for at least 350 time units to achieve statistical convergence. The spatial and temporal resolution of the simulations were rigorously assessed and were found to be adequate (Sandberg *et al.*, 2012).

RESULTS

Instantaneous contours of the streamwise density gradient are shown for the near-nozzle region in figure 2 to visualize the turbulent flow exiting the long pipe into the

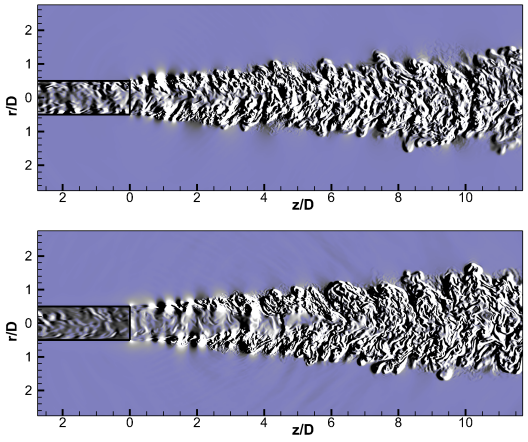

Figure 2. Instantaneous contours of streamwise density gradient near the nozzle; top: M45c1L with levels $[-1\times10^{-3};\,1\times10^{-3}]$, bottom: M84c2L with levels $[-5\times10^{-3};\,5\times10^{-3}]$.

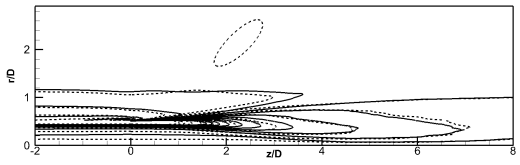

Figure 3. Contour lines of time- and azimuthally averaged azimuthal vorticity component for cases M84c2L (solid) and M45c1L (dashed) with 21 levels for range $[-4;\,4]$.

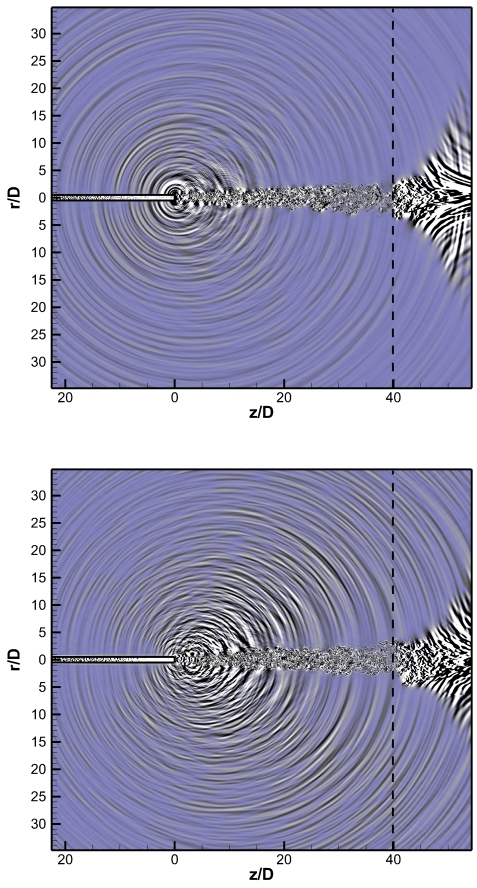

Figure 4. Instantaneous contours of dilatation field for azimuthal plane $\Theta = 0^\circ, 180^\circ$; top: M45c1L with levels $[-1\times10^{-4};1\times10^{-4}]$, bottom: M84c2L with levels $[-5\times10^{-4};5\times10^{-4}]$.

co-flow. The cases M45c1L and M84c2L are compared to each other because both feature roughly the same velocity difference between jet exit and co-flow velocity, i.e. a non-dimensional velocity excess of $\lambda \approx 4$. Sandberg *et al.* (2012) showed that the turbulence statistics at the nozzle exit could be collapsed with profiles in the fully developed region, thus the flow exiting the pipe can be considered fully developed and therefore constitutes a well defined turbulent upstream condition suitable for direct noise computations. For either case, it can be observed that the initial shear layers of the jet are turbulent and do not need to undergo a laminar-turbulent transition, resulting in a rapidly developing turbulent jet. Figure 2 also reveals significant differences between the two cases, such as (the expected) significantly increased amplitudes of the density gradient in the higher Mach number case, an apparent higher coherence of the shear layer structures in the case with higher jet exit Mach number, and seemingly different spreading rates. The latter observation, however, appears to be associated with the particular time instant at which the two cases are compared as plotting the time- and azimuthally averaged azimuthal vorticity component (fig. 3) reveals that the axial growth of the two jet cases is very similar.

For a qualitative impression of the resulting acoustic field, instantaneous contours of the dilatation field in the entire computational domain are shown in Fig. 4. Sound waves can be observed emanating from the end of the pipe ($z/D = 0$) and from the jet core. Importantly, no interference of the acoustic field from boundary reflections can be detected, which is particularly encouraging given the very small contour levels chosen ($\pm1\times10^{-4}$ for the M45c1L case). For the higher Mach number case M84c2L, the noise radiation is considerably more directive than for the lower Mach number case, with the highest sound radiation intensity observed at roughly $\theta = 40^\circ$, where θ is defined with respect to the streamwise direction. For both cases, upstream radiating noise emanating from the nozzle lip, although more weakly, can be detected. Overall, from these figures it would appear as if for the lower jet Mach number case it will be very difficult to extract the jet noise component of the farfield noise in order to investigate the Mach number scaling.

For that reason, the far field noise generated by the turbulent jet was investigated with a phased array technique in order to quantitatively separate the jet mixing noise from any other sources of noise that might be present, e.g. nozzle lip noise. Although such techniques have been available for many years, successful application to LES and DNS data has often been prevented by a combination of two factors: the lack of far-field data and the lack of sufficient time history (record length) to obtain adequate accuracy in the required statistical quantities, such as the spectral density and cross-spectral density of the radiated unsteady pressure.

In the current study, a polar array of virtual microphones has been located at 20 jet nozzle diameters from the nozzle, having ascertained that the field is obeying the

inverse square law at this radius, without any significant reflections from the DNS domain boundaries. The DNS record length, in excess of 350 convective time units for all cases, permits the number of averages for the cross-spectral density to be of order 100 with a filter separation, expressed as a Strouhal number based on the nozzle diameter, of 0.1. A microphone spacing of 0.5 degrees is used over an aperture of 140 degrees to 10 degrees to the jet axis (i.e. 40 to 170 degrees to the 'intake' axis), although even finer spacing is available, if required. To assess the contribution of individual azimuthal modes to the overall noise the pressure PSDs were Fourier decomposed in the circumferential direction. This azimuthal data has then been analyzed with a recently developed phased array code, named AFINDS and described in more detail in Tester & Gabard (2012), which, in addition to the usual imaging capability, is able to extract a 'noise source breakdown' using a model in which the jet mixing noise is represented by one or two distributed axial sources. In the current work only one jet-noise source is used plus two nozzle-based sources, each represented by a simple point-source. Using AFINDS to compare case M84c2L to another DNS case using the same flow parameters and overall set-up, but without the liner boundary condition, it has been possible to elucidate the effect of the acoustic liner model on the respective contributions from the nozzle based and the jet mixing noise sources. The results obtained from the noise source breakdown showed that the liner only marginally affects the axisymmetric mode while being very effective at reducing nozzle-based noise contributions in the higher azimuthal modes (Sandberg & Tester, 2014).

In the present paper, the focus is on investigating the Mach number scaling of the jet noise component for all jet Mach numbers considered. The resulting Mach number scaling is shown in figure 5 for a normalized PSD summed over the axisymmetric mode $m = 0$ and the higher azimuthal modes $m = 1$, $m = 2$, and $m = 3$ at 90° and for a Strouhal number of $St_D = 1$. This frequency was chosen because the acoustic liner boundary condition used inside the pipe was set to resonate at this frequency and it was therefore expected that the jet noise component would be least contaminated by internal noise at this frequency. Note that the PSD is plotted versus the Mach number based on the centreline velocity.

In figure 5, the PSD at 90° and distance 20 diameters from the nozzle for $St_D = 1.0$ is normalized by $(1 - u_{co}/u_{CL})^5$ to account for jet noise co-flow effects. Note that four data points are included, one each for the cases M45c1L, M62c15L, M8c1L and M8c2L, with the latter two being at the same location of the horizontal axis. The scaling obtained from DNS directly corresponds approximately to a M^5 scaling, indicating that in addition to jet mixing noise there are other noise sources present, such as, e.g., nozzle-lip noise. However, when performing the source breakdown using AFINDS to separate out the jet-noise source, the expected Mach number scaling of M^8 is obtained, particularly accurately for $M_{jet} > 0.64$, a well established scaling law for isothermal jet noise, both experimentally and theoretically. This result is very encouraging in two respects. Firstly, it demonstrates the capability of AFINDS to extract the jet-noise source from the overall acoustic field, and secondly it shows that the series of DNS solutions is capturing the expected physics.

In order to produce the following figures the far-field pressure field was decomposed into azimuthal Fourier

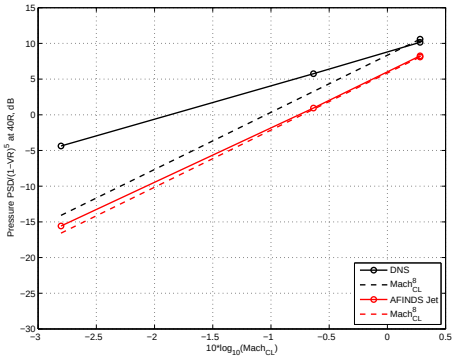

Figure 5. Mach number scaling of the jet noise component at 90° for $St_D = 1.0$; open black symbols with solid line represent DNS data, dashed lines show M^8 scaling (based on jet axis velocity), and red open symbols with solid line are the AFINDS fit for the jet noise component of the overall noise field.

modes in order to investigate the Mach number scaling of the individual circumferential modes. In figure 6 the total pressure PSD, displayed the same way as in figure 5 and from the same spatial location, is shown for modes $m = 0$, $m = 1$ and $m = 3$. The picture for $m = 0$ is very similar to that of the total noise field, i.e. the scaling of the raw data is nowhere close to M^8 scaling, while the jet-noise source extracted from the data using the noise source breakdown technique agrees very well with the theoretical prediction. However, when considering $m = 0$ only, a near-exact M^8 scaling is obtained across all simulated Mach numbers, implying that when considering all Fourier modes there are some contributions from higher modes at the lowest jet Mach number that cause the scaling to slightly deviate from an eighth power law (c.f. fig. 5). When investigating the behaviour of $m = 1$, several observations can be made. First, the raw DNS data now displays a M^8 scaling when considering only cases M62c15L, M8c1L and M8c2L. This implies that the liner boundary conditions used in the DNS are removing most of the internal noise sources and therefore the overall farfield noise is mainly comprised of jet mixing noise in these cases. At the lowest jet Mach number simulated, extracting the jet noise source using AFINDS is required in order to obtain a Mach number scaling with approximately eighth power. For $m = 3$, the behaviour described for $m = 1$ is even clearer, with the DNS raw data coming even closer to an eighth power law scaling (implying even better performance by the liner boundary conditions) and the AFINDS jet noise source exhibiting a nearly perfect M^8 scaling across all jet Mach numbers investigated.

The crucial and, to the authors' knowledge formerly unknown, finding is that it appears as if all azimuthal Fourier modes adhere to the same Mach number scaling.

In order to assess whether the Mach number scaling of the individual azimuthal modes is not particular to $St_D = 1$, two additional Strouhal numbers were investigated, one significantly lower, $St_D = 0.2$, corresponding to the peak in the power spectral density, and one significantly higher, $St_D = 1.4$. The results are shown in figures 7 and 8. The results for the lower frequency are very similar to those at $St_D = 1$. For the axisymmetric mode, it is necessary to extract the jet noise source using AFINDS in order to find a Mach number scaling with an exponent close to eight.

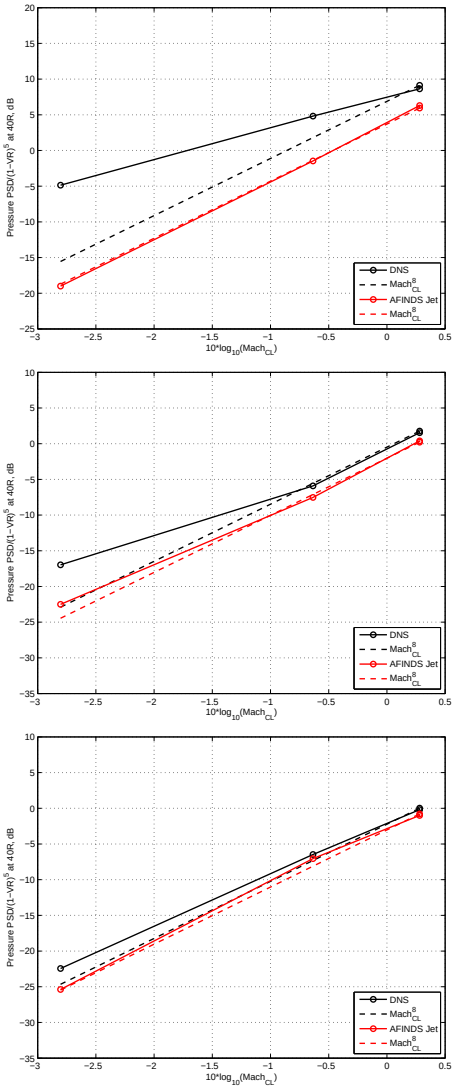

Figure 6. Mach number scaling of the jet noise component at 90° for $St_D = 1.0$ for azimuthal Fourier modes $m = 0$, $m = 1$ and $m = 3$ (from top to bottom); symbols and lines as described in caption of figure 5.

The AFINDS algorithm did not achieve convergence for case M45c1L due to the low level of jet noise at this frequency relative to the two nozzle-based sources. However, the other data points lie on the expected line. For higher modes (mode $m = 1$ is shown), using the raw DNS data, M^8 scaling can only be observed for the higher jet Mach number cases. Looking at the jet noise source only, extracted with AFINDS, excellent agreement with the expected M^8 scaling is found, in fact even better as for $St_D = 1$.

At the higher frequency $St_D = 1.4$ (figure 8), the picture is not as clear as for the lower Strouhal numbers considered. For the axisymmetric mode, the raw DNS data does not give a constant Mach number scaling over the range of jet Mach numbers simulated and for no segment is close to an eighth power law. When isolating the jet noise source with AFINDS, the Mach number scaling between cases with $M_{jet} = 0.45$ and $M_{jet} = 0.8$ is close to M^8. However, the case M62c15L does not follow the same trend and requires further investigation. For the first azimuthal mode

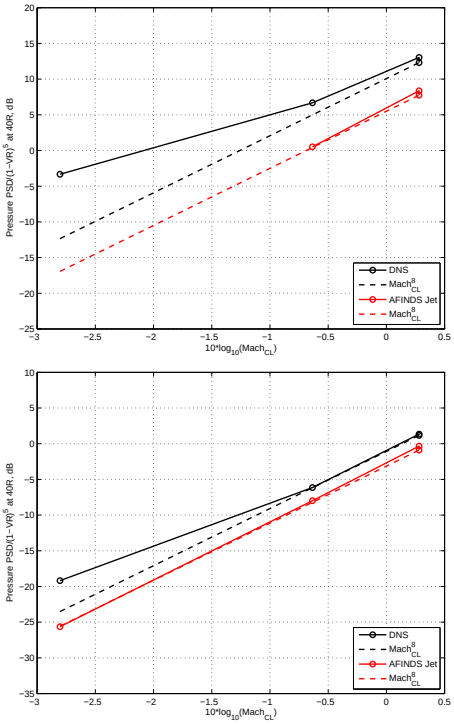

Figure 7. Mach number scaling of the jet noise component at 90° for $St_D = 0.2$ for azimuthal Fourier modes $m = 0$ (top) and $m = 1$ (bottom); symbols and lines as described in caption of figure 5.

$m = 1$, the acoustic liner boundary condition again appears to serve its purpose well and the data obtained from the raw data and from AFINDS produce nearly the same line, except for an amplitude of approximately 4 dB for the DNS data. Despite being very similar, both do not yield a consistent scaling over the entire M_{jet} range and exhibit a scaling with an exponent lower than eight. Why the Mach number scaling of the jet noise source changes for higher frequencies is currently under investigation.

Conclusions

A series of direct numerical simulations of fully turbulent flow exiting a long pipe were conducted at target Reynolds number, based on jet exit velocity at the axis, of $Re_{jet} = 8,000$, for varying jet exit and co-flow Mach numbers.

The main objective of the work was to investigate the Mach number scaling of the jet noise for individual azimuthal Fourier modes. In order to assess pure jet mixing noise, a number of challenges had to be overcome. Firstly, based on previous experience with DNS of pipe-jet configurations, several key features were required to be included in the simulations to produce as clean a jet noise field as possible. To suppress possible internal noise sources emanating from the pipe exit and contaminating the acoustic far field, an acoustic liner model was applied to the interior nozzle walls. In addition, the turbulent inflow generation technique was modified to be free of velocity fluctuations in the axisymmetric mode. Furthermore, despite the DNS producing a much cleaner jet noise field than earlier simulations, the use of a source breakdown code was essential in

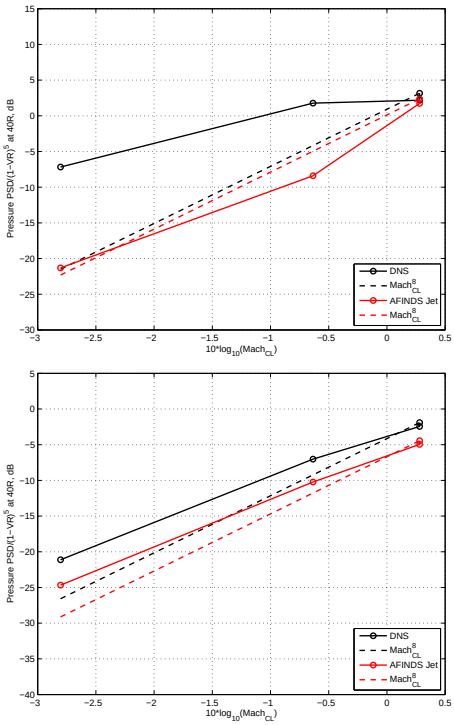

Figure 8. Mach number scaling of the jet noise component at 90° for $St_D = 1.4$ for azimuthal Fourier modes $m = 0$ (top) and $m = 1$ (bottom); symbols and lines as described in caption of figure 5.

order to isolate the jet noise source from the overall noise field, in particular for the axisymmetric mode $m = 0$.

It is found that the overall jet noise sources, i.e. the sum of the azimuthal modes, shows the expected M^8 scaling with the centreline jet Mach number when accounting for co-flow effects by scaling the results with $(1 - u_{co}/u_{CL})^5$. More importantly, the DNS results also suggest that the individual azimuthal modes exhibit the same scaling, at least for Strouhal numbers up to $St_D = 1$. At higher frequencies, a consistent scaling over the entire M_{jet} range could not be found and the exponent is lower than eight. The reason for this behaviour is still unknown and is the subject of a current investigation. To date, only the far-field pressure at 90° has been considered, as the M^8 scaling is well documented for this angle. However, the DNS data will also allow an investigation of Mach number scaling for other angles in future work.

REFERENCES

Bogey, C. & Bailly, C. 2010 Influence of nozzle-exit boundary-layer conditions on the flow and acoustic fields of initially laminar jets. *J. Fluid Mech.* **663**, 507–538.

Bogey, C., Marsden, O. & Bailly, C. 2011 Large-Eddy simulation of the flow and acoustic fields of a Reynolds number 105 subsonic jet with tripped exit boundary layers. *Phys. Fluids* **23**, 035104.

Crighton, DG, Williams, J.E.F. & Cheeseman, IC 1976 The outlook for simulation of forward flight effects on aircraft noise. *AIAA J.* **530** (76).

Gutmark, E. & Ho, C.M. 1983 Preferred modes and the spreading rates of jets. *Phys. Fluids* **26**, 2932.

Hussain, A. & Zedan, MF 1978 Effects of the initial condition on the axisymmetric free shear layer: effects of the initial momentum thickness. *Phys. Fluids* **21**, 1100.

Michalke, A. & Michel, U. 1979*a* Prediction of jet noise in flight from static tests. *J. Sound Vib.* **67** (3), 341–367.

Michalke, A. & Michel, U. 1979*b* Relation between static and in-flight directivities of jet noise. *J. Sound Vib.* **63**, 602–605.

Olivetti, S., Sandberg, R. D. & Tester, B. J. 2015 Direct Numerical Simulation of Turbulent Flow with an Impedance Condition. *J. Sound Vib.* **344**, 28.

Raman, G., Zaman, K.B.M.Q. & Rice, E.J. 1989 Initial turbulence effect on jet evolution with and without tonal excitation. *Phys Fluids A: Fluid Dynamics* **1**, 1240.

Sandberg, R.D., Pichler, R., Chen, L., Johnstone, R. & Michelassi, V. 2015 Compressible Direct Numerical Simulation of Low-Pressure Turbines: Part I – Methodology. *J. Turbomachinery* **137**, 051011–1–051011–10.

Sandberg, R.D., Suponitsky, V. & Sandham, N.D. 2012 DNS of compressible pipe flow exiting into a coflow. *Int. J. Heat Fluid Fl.* **35**, 33–44.

Sandberg, R. D. 2014 DNS of Turbulent Round Jets Using Acoustically Lined Canonical Nozzles. *Proceedings of the AFMC, Paper 143* 19th Australasian Fluid Mechanics Conference, Melbourne, Australia.

Sandberg, R. D. & Sandham, N. D. 2006 Nonreflecting zonal characteristic boundary condition for direct numerical simulation of aerodynamic sound. *AIAA J.* **44** (2), 402–405.

Sandberg, R. D., Suponitsky, V. & Sandham, N.D. 2011 DNS of fully turbulent jet flows in flight conditions including a canonical nozzle. *AIAA Paper 2011–2918*.

Sandberg, R. D. & Tester, B.J. 2014 DNS of a turbulent jet issuing from an acoustically lined pipe. *Proceedings of the IUTAM Symposium on Advances in Computation, Modeling and Control of Transitional and Turbulent Flows* .

Sandberg, R. D. & Tester, B. J. 2012 Application of a Phased Array Technique to Fully Turbulent Subsonic Jet Data Obtained with DNS. *AIAA Paper 2012–2613*.

Shur, M.L., Spalart, P.R. & Strelets, M.K. 2010 Reprint of: LES-Based Evaluation of a Microjet Noise Reduction Concept in Static and Flight Conditions. *Procedia IUTAM* **1**, 44–53.

Tam, Christopher K.W. & Auriault, Laurent 1996 Time-domain impedance boundary conditions for computational aeroacoustics. *AIAA J.* **34** (5), 917–923.

Tanna, H.K. & Morris, P.J. 1977 In-flight simulation experiments on turbulent jet mixing noise. *J. Sound Vib.* **53** (3), 389–405.

Tester, B. J. & Gabard, G. ad Ricoup, T. 2012 Extracting engine noise source levels from phased array measurements with improved internal source models and evaluation against DNS-generated jet noise data. *AIAA Paper 2012–2272*.

Tester, B. J. & Sandberg, R. D. 2013 Application of a phased array technique to DNS-generated turbulent subsonic jet data: source identification and comparison with an analytic model. *AIAA Paper 2013–2235*.

Zaman, K. B. M. Q. 1985 Effect of initial condition on subsonic jet noise. *AIAA J.* **23**, 1370–1373.